



# New Chemical Constituents from the Leaves and Twigs of *Holoptelea integrifolia*

Sukee Sukdee<sup>1</sup>, Puttinan Meepowpan<sup>2</sup>, Narong Nantasaen<sup>3</sup>, Siriporn Jungsuttiwong<sup>4</sup>, Nuttapon Yodsin<sup>4</sup> and Wilart Pompimon<sup>1\*</sup>

<sup>1</sup>Laboratory of Natural Products, Faculty of Science and Center for Innovation in Chemistry, Lampang Rajabhat University, Lampang – 52100, Thailand; Pompimon.wilart@gmail.com

<sup>2</sup>Department of Chemistry, Center for Innovation in Chemistry, Faculty of Science, Graduate School, Chiang Mai University, 239 Huay Kaew Road, Chiang Mai – 50200, Thailand

<sup>3</sup>The Forest Herbarium, Department of National Park, Wildlife and Plant Conservation, Ministry of Natural Resources and Environment, Bangkok – 10220, Thailand

<sup>4</sup>Center for Organic Electronic and Alternative Energy, Department of Chemistry and Center of Excellence for Innovation in Chemistry, Faculty of Science, Ubon Ratchathani University, Ubon Ratchathani – 34190, Thailand

## Abstract

Phytochemical examination on the different extracts of leaves and twigs of *Holoptelea integrifolia* (*H. integrifolia*) were carried out with varied polar organic solvents. The chemical constituents of crude extracts were separated and isolated by using chromatography technique and characterized by using spectroscopies of <sup>1</sup>H, <sup>13</sup>C and 2D NMR. Two known compounds, the stigmasterol (**1**) and octamethylcyclohexane-1,4-dione (**2**), and one new compound, di-myo-inositol (**3**) were isolated and characterized. Chemical constituent **2** and **3** has been reported for the first time in *H. integrifolia*; in addition, constituent **3** was new phytochemical finding.

**Keywords:** Di-myo-inositol, *Holoptelea*, *H. integrifolia*, Octamethylcyclohexane-1,4-dione

## 1. Introduction

There are 15 genera and 200 species in the family ulmaceae which could be found in Thailand. *H. integrifolia* Roxb. belong to the family ulmaceae<sup>1-3</sup>. It has been traditionally used since ancient times. Barks and leaves were used as bitter, astringent, anthelmintic, acrid termogenic, digestive, laxative, carminative, antibacterial, antimicrobial, antitumour, depurative, repulsive, antidiabetic, antiinflammatory and in rheumatism. Extracts of various parts from *H. integrifolia* has been proven beneficial for the treatment disease in agreement to its ethnomedical use. It has been used inpatients to cure inflammation, gastritis,

dyspepsia, colic, intestinal worms, vomiting, wound healing, leprosy, diabetes, hemorrhoids, diarrhea, polyuria, helminthiasis, tuberculosis, fistula, flatulence, vitiligo, filariasis, skin diseases, dysmenorrhea and rheumatism, etc.<sup>4-11</sup>. The chemical constituents isolated from *H. integrifolia* include carbohydrates, alkaloids, terpenoids, flavonoids, sterols, saponins, tannins and proteins, such as holoptelin A-B, epifriedelin, friedelin, lupeol, pesitosterol, 2-aminonaphthaquinone, aquinone, eolellagic acid, asitosterol-D-glucoside, epifriedelinol, hexacosanol, octacosanol, taamyrin, yramyrin, hederagenin, stigmasterol, friedel-1-en-3-one, butulinic acid and botulin<sup>12-19</sup>. Herein, we report chemical constituents of leaves and twigs from *H. integrifolia*,

\*Author for correspondence

namely stigmasterol (**1**)<sup>20</sup>, octamethylcyclohexane-1,4-dione (**2**)<sup>23</sup> and di-myoinositol (**3**). The compound **3** was isolated for the first time from *H. integrifolia*.

## 2. Materials and Methodology

### 2.1 Experimentation

Chromatography technique was used for the separation and isolation compounds. Investigation the melting points in degree Celsius ( $^{\circ}\text{C}$ ) were recorded on a digital Electro thermal melting apparatus. The FTIR spectra reported major bands ( $n_{\text{max}}$ ) (Shimadzu 8900).  $^1\text{H}$  and  $^{13}\text{C}$  NMR spectra were determined in  $\text{CDCl}_3$  and  $\text{D}_2\text{O}$  solution. Tetramethylsilane (TMS) was used as reference of the chemical shifts was the standard appear down field at  $\delta$  0.00 ppm, were recorded in  $\delta$  values; using a NMR spectrometers (Bruker AV 400) in order to one and two dimensional evaluation. The ESI-MS spectra were measured with a micro hybrid quadrupole/time-of-flight (Q-TOF) mass spectrometer; for positive ions mass was reported by a Finnegan Polaris Q mass spectrometer at 70 eV. ECD calculations were on compounds with the time dependent DFT method at CAM-B3LYP/6-311++G level. All procedure calculations are carried out the Gaussian09 program package, were plotted with 0.25 eV.<sup>27</sup>

### 2.2 Material

The Leaf and branches of *H. integrifolia* was compiled in Lampang Province of Thailand in January 2012, identified by Mr. Narong Nantasean.

### 2.3 Extraction and Isolation

6.50 kg of leaves and branches of *H. integrifolia* were dried out with air-dried, then grinded to powder which were consecutive percolated prior with organic solvents solution; n-hexane, ethyl ethanoate and methyl alcohol (20 L  $\times$  3 days  $\times$  4 times), at room temperature, and filtered respectively. Combination filtrates were evaporated to dry under reduced pressure were resulted in the residues, n-hexane (17.1 g), ethyl ethanoate (33.5 g) and methyl alcohol (250.0 g), in order. 16.0 g of n-hexane extract was further fractionated via chromatography technique with varying the organic solvent conditions from weak to strong polarity i.e.,

n-hexane, ethyl ethanoate and methyl alcohol. The filtrates were evaporated to give 9 fractions. Then, 3.55 g of  $F_4$  was eluted with ethyl acetate/hexane (3/7) and the solvent was evaporated resulting in a brown semisolid, further recrystallized with ethyl acetate/ethanol (7/3) to afford the pure colorless needle crystals and which was identified as stigmasterol (**1**). 33.0 g of crude extract of ethyl acetate was fractionated under the same method and the gradient conditions, to afford 15 fractions. 3.0 g of brown semisolid of  $F_{14}$  was re-chromatographed and eluted with 40% ethyl acetate/methanol, sub-fraction  $F_{14-4}$  was obtained as white crystals. It was collected and identified as compound **2**. While 50.0 g of crude extract of methanol was fractionated with same method but eluted under different gradient conditions: hexane/ethyl acetate, ethyl acetate/methanol and methanol to obtain 13 fractions. 5.35 g of  $F_9$  was fractionated with chromatography technique, eluted with methanol, followed by solvent evaporation, recrystallized with ethanol/water (8/2) to form pure white needle crystals, and identified as compound **3**.

## 3. Results

### 3.1 Stigmasterol (1)

Colorless needle crystal; mp: 163-164  $^{\circ}\text{C}$ ; IR (KBr)  $n_{\text{max}}$ : 3460, 2955, 2870, 1650, 1465, 1377, 1050  $\text{cm}^{-1}$ . The  $^1\text{H}$  NMR:  $\delta$  0.72 (3H, s, H-28), 0.81 (3H, d,  $J = 5.0$  Hz, H-27), 0.85 (3H, d,  $J = 5.0$  Hz, H-26), 0.87 (3H, t,  $J = 5.0$ , H-24), 0.94 (3H, d,  $J = 10.0$  Hz, H-19), 1.06 (3H, s, H-29), 4.01 (1H, qui,  $J = 5.0$  Hz, H-3), 5.03 (1H, dd,  $J = 10.0, 10.0$  Hz, H-20) 5.16 (1H, dd,  $J = 10.0, 10.0$  Hz, H-21), 5.62 (1H, brd, H-6);  $^{13}\text{C}$  NMR:  $\delta$  12.03 (C-23), 12.26 (C-29), 18.98 (C-28), 19.45 (C-27), 20.27 (C-26), 21.10 (C-11), 24.42 (C-15), 25.41 (C-23), 28.88 (C-16), 29.14 (C-25), 31.77 (C-8), 31.85 (C-7), 31.88 (C-2), 36.14 (C-10), 38.21 (C-1), 39.37 (C-12), 40.49 (C-18), 41.67 (C-4), 41.70 (C-13), 45.83 (C-22), 51.23 (C-9), 56.02 (C-17), 56.70 (C-14), 72.95 (C-3), 125.72 (C-6), 129.31 (C-21), 137.22 (C-20), 138.26 (C-5).

### 3.2 Octamethylcyclohexane-1,4-dione (2)

A white crystal, IR (KBr)  $n_{\text{max}}$ : 2903, 2853, 1590  $\text{cm}^{-1}$ ;  $^1\text{H}$  NMR :  $\delta$  1.74 (24H, s,  $8\times\text{CH}_3$ );  $^{13}\text{C}$  NMR :  $\delta$  23.01 ( $8\times\text{CH}_3$ ), 47.55 (C-2), 48.06 (C-3), 48.41 (C-5), 48.62

(C-6), 181.46 (C-1/C-4); ESIMS  $[M+NH_4^++H^+]$  at  $m/z$  243,  $C_{14}H_{24}O_2$  (cal. for  $C_{14}H_{24}O_2$ , 224).

### 3.3 Di-myo-inositol (3)

A white needle crystal; mp: 228-229 °C; IR (KBr)  $n_{max}$ : 3400, 2935, 2840, 1422, 1367, 1150, 1117, 1050, 1004  $cm^{-1}$ ;  $^1H$  NMR: d 3.12 (2H, t,  $J = 10.0$  Hz, H-1/H-1'), 3.37 (4H, dd,  $J = 5.0, 10.0$  Hz, H-3/H-3'), 3.47 (4H, t,  $J = 10.0$  Hz, H-2/H-2'), 3.90 (2H, t,  $J = 5.0$  Hz, H-4/H-4');  $^{13}C$  NMR: d 71.11 (C-3/C-3'), 72.16 (C-4/C-4'), 72.37 (C-2/C-2'), 74.33 (C-1/C-1'); ESIMS  $[M+2H^+]$  at  $m/z$  406,  $C_{22}H_{28}O_7$  (cal. for  $C_{22}H_{28}O_7+H$ , 404) (Table 1).

**Table 1.**  $^1H$  NMR and  $^{13}C$  NMR spectral data,  $^1H$ - $^{13}C$  long-rang and  $^1H$ - $^1H$  correlations of compound **3** in  $D_2O$  obtained by HMBC and COSY

Comparison of NMR data of compound <b>3</b>				
Position	$\delta_C$ (ppm)	$\delta_H$ (ppm)	COSY	HMBC
1	74.33	3.12, t(10.0)	2	1', 2
2	72.37	3.47, t(10.0)	1, 3	1, 3
3	71.11	3.37, t(10.0, 5.0)	2, 4	2
4	72.16	3.90, t(5.0)	3	1, 2, 3
1'	74.33	3.12, t(10.0)	2'	1, 2'
2'	72.37	3.47, t(10.0)	1', 3'	1', 3'
3'	71.11	3.37, t(10.0, 5.0)	2', 4'	2'
4'	72.16	3.90, t(5.0)	3'	1', 2', 3'

<sup>a</sup>Assignments made on the basis of NMR; <sup>b</sup>Chemical shift values are in (ppm); <sup>c</sup>Coupling constants are in Hz.

## 4. Discussion

Three compounds from *H. integrifolia*, were isolated and structural identified by using spectroscopic techniques. They were found to be stigmasterol (**1**), octamethylcyclohexane-1,4-dione (**2**) and di-myo-inositol (**3**). Compound (**1**) and (**2**) were reported for the first time from crude ethyl acetate extract and compound (**3**) as the new compound from crude methanol extract of *H. integrifolia* (Figure. 1).

Compound **1** was isolated as colorless needle crystal, mp 163-164 °C, assigned the molecular  $C_{29}H_{48}O$ . Infrared spectroscopy spectra presented the broad absorption band of a hydroxyl group at  $3460\text{ cm}^{-1}$ . Absorptions appeared at  $2955$  and  $2870\text{ cm}^{-1}$  were affected from C-H stretching. The C-H bending showed as weak absorptions at  $1465$  and  $1377\text{ cm}^{-1}$ . The weak absorption of C=C stretching appeared at  $1650\text{ cm}^{-1}$ . The stretching vibration of C-O was medium intense band at  $1050\text{ cm}^{-1}$ . Chemical constituent was further confirmed by investigation of the nuclear magnetic resonance techniques. Which, the comparative relation of  $^1H$  and  $^{13}C$  NMR spectra were observed similar with the previously report<sup>20</sup>. These were data in accordance with those of stigmasterol (**1**)<sup>20</sup> (Figure 2, 3).

Compound **2** was recrystallized a white crystal. ESIMS gave mass ion peak  $[M+NH_4^++H^+]$   $m/z$  243, corresponded the molecular  $C_{14}H_{24}O_2$  (cal.  $C_{14}H_{24}O_2$ , 224). The molecular ion  $[M+NH_4^++H^+]$  spectra appeared at 243; it changed to the molecular ion 165 arising from  $m/z$  243 by further loosed of methyl and carbon monoxide, for  $m/z$  156 was originated the 2-methyl-3-oxoallylium by an elimination molecule. Structure was confirmed from the spectrum at  $m/z$  378 and 379, suggestion of an

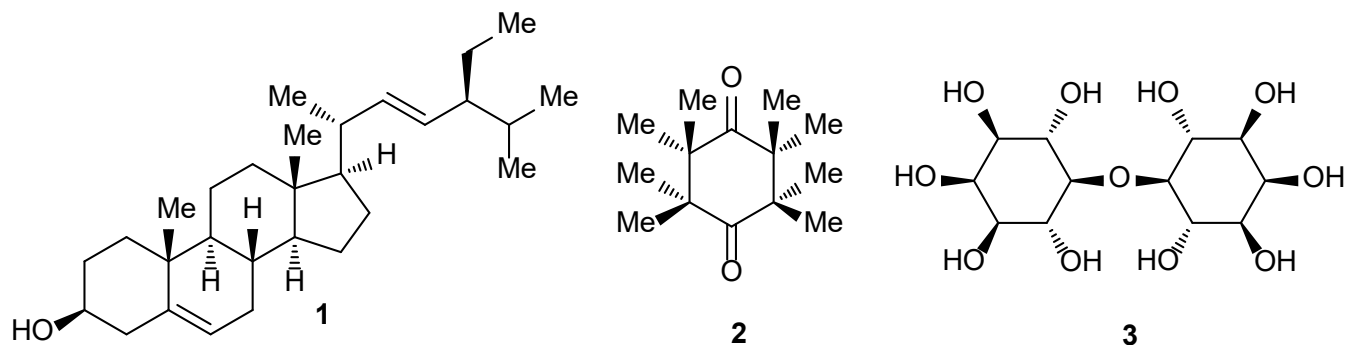


**Figure 1.** Structure of compounds isolated from *H. integrifolia* (roxb.).

additional hexamethylcyclobutanol and hydronium attached to the primary carbocation and carbonyl group respectively. Molecular ions peak appeared in the spectrum at  $m/z$  380 and 381; suggestion with the reaction of molecular by 1,3-hydride shift to carbonyl group which give a carbocation followed an additional hexamethylcyclobutanol and protonated in order. IR spectrum displayed bands to carbonyl functionalities at  $1590\text{ cm}^{-1}$ . The stretching vibrations of C–H are also appeared at  $2903$  and  $2853\text{ cm}^{-1}$ . Chemical constituent of **2** was further supported by 1D and 2D NMR experimentation.  $^1\text{H}$  NMR spectrum displayed signals for protons at  $\delta$  1.74 (24H, s, H-Me) were assigned to methyl protons adjacent to quaternary carbon.  $^{13}\text{C}$  NMR spectrum of compound **2** showed 6 signals of six carbons. Signals at  $\delta$  181.46 were assigned to carbonyl carbons of ketone groups. Methyl carbon showed at  $\delta$  23.01 ppm. Signals at  $\delta$  47.55, 48.06, 48.41 and

48.62 were indicated quaternary carbon. Asymmetric structure supposes arising from single bonding rotation in a molecule. The angles and conformation have energy differentia. Therefore, structure had asymmetries affecting nuclear magnetic resonance of position carbon atom; spectrum of  $^{13}\text{C}$  were nonequivalent<sup>21,22</sup>. The HMBC spectra demonstrated the correlation of methyl proton H-Me to C-1 indicating the methyl connected at C-1 and confirmed the position of a carbonyl carbon. The correlation of methyl proton H-Me to C-Me indicating the methyl connected at C-Me and confirmed the position of a methyl nearby. These data were in accordance with those of octamethylcyclohexane-1,4-dione (**2**)<sup>23</sup> (Figure 2, 3).

Compound **3** was obtained as a white needle crystal; mp  $228\text{--}229^\circ\text{C}$ . The ESIMS was  $[\text{M}+2\text{H}^+]$  at  $m/z$  406, in accordant with the molecule  $\text{C}_{22}\text{H}_{28}\text{O}_7$  (cal. for  $\text{C}_{22}\text{H}_{28}\text{O}_7+\text{H}$ , 404). The spectrum of  $[\text{M}+\text{NH}_4^+]$  was at

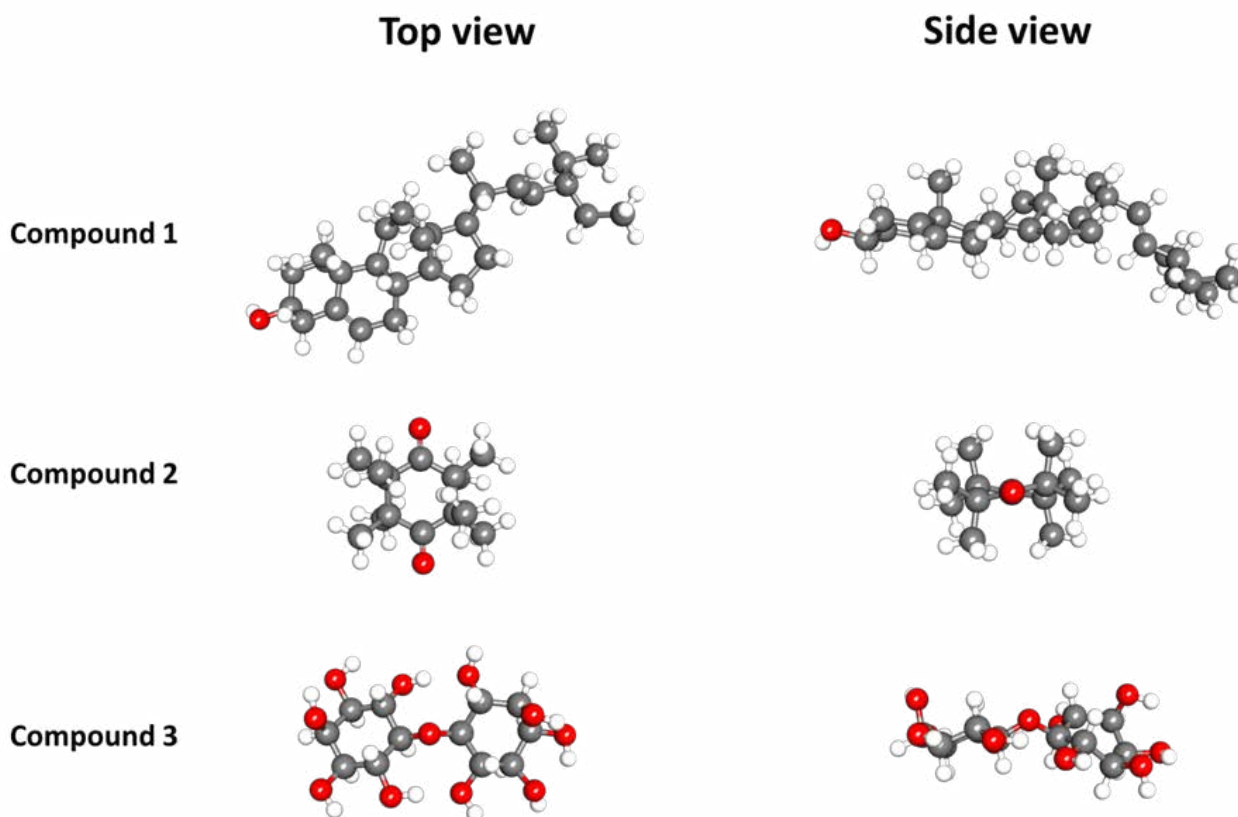


**Figure 2.** The optimized structures of compound 1-3.

$m/z$  359; there are the ions  $m/z$  355 and 354 flows from  $m/z$  359 by further loss of hydrogen atoms. Spectra also contains the mass  $m/z$  294, owing to loss of water and formaldehyde,  $m/z$  282 corresponds to loss of an ethane-1,2-diol. Structural assignment was further supported by mass  $m/z$  304; originate eradication water and hydrogen atoms, which feature  $m/z$  302 and 301, conformity eliminated hydrogen atoms, further loss of the myo-inosital moiety from  $m/z$  342 gives rise  $m/z$  178. These two ions are higher than like ions observed in the mass spectra at  $m/z$  416 and 399, suggesting of an additional 2-hydroxypropanal and 2-hydroxyacetaldehyde attached to the O-hydroxyl of di-myo-inosital respectively. These spectra appeared as fragmented ions in the mass spectra. IR spectrum presents peak at  $3400\text{ cm}^{-1}$  which was characterized as hydroxyl group. The secondary alcohol absorption was observed at  $1050$  and  $1004\text{ cm}^{-1}$  and were identical to the C–O stretching; but, the C–O stretching of ether showed medium absorption bands at  $1150$  and  $1117\text{ cm}^{-1}$ . The  $\text{sp}^3$  hybridized C–H bonds were exhibiting asymmetric stretching vibration; therefore, absorption then appeared at red-shift to low frequencies, giving rise to highly resolved spectra. Strong absorption sat  $2935$  and  $2840\text{ cm}^{-1}$  were characterized by C–H stretching, while its corresponding bending vibrations appeared at  $1422$  and  $1367\text{ cm}^{-1}$ . Chemical constituent of **3** was further clarified by 1D and 2D analyses.  $^1\text{H}$  NMR spectrum showed the methine protons at  $\delta$  3.12 (2H, t,  $J=10\text{ Hz}$ , H-1, 1') that were assigned to methine protons adjacent to oxygen of ether group. A doublet of doublet of methine protons was observed at  $\delta$  3.37 (4H, dd,  $J=10.0, 5.0\text{ Hz}$ , H-3, 3'). The resonances at  $\delta$  3.47 (4H, t,  $J=10\text{ Hz}$ , H-2, 2') and  $\delta$  3.90 (2H, t,  $J=5.0\text{ Hz}$ , H-4, 4') were a methine proton. The  $^{13}\text{C}$  NMR spectra exhibited the resonances of a methine carbons  $\delta$  74.33 (C-1, C1'), 72.37 (C-2, 2'), 72.16 (C-4, 4') and 71.11 (C-3, 3'). Homo-nuclear correlation spectroscopic (COSY) spectra presented coupling correlations thoroughly with the succession of H-1 to H-2, H-2 to H-3, and H-3 to H-4; H-1' to H-2', H-2' to H-3', and H-3' to H-4' for the connectivity of the protons to the structure. HMBC correlation of H-1 to C-2; H-2 to C-1, 3; H-3 to C-2 and H-4 to C-1, 2, 3; H-1' to C-2'; H-2' to C-1', 3'; H-3' to C-2' and H-4' to C-1', 2'; were confirmed to hexacyclic ring, and then relationship of H-1 to C-1' and H-1' to

C-1 were clearly indicated by the dimer hexacyclic ring compound as shown as Figure. 2. The connection in the middle of the torsion angle and vicinal coupling constant  $^3J$  was presented in theory by the Karplus equation:  $^3J(\text{HH}) = P_1 \cos^2\phi + P_2 \cos\phi + P_3 + \sum \Delta\chi_i \{P_4 + P_5 \cos^2(\xi_i\phi + P_6|\Delta\chi_i|)\}^{24}$ . Therefore, the comparative form at H-1 and H-2, H-2 and H-3, ascertained correlation with  $^3J_{1,2; 2,3}$  H–C–C–H (10 Hz) coupling constants, that indicated hydrogen atoms on contrary sides a dihedral angle of  $170.3^\circ$  assignment to the trans-configuration. Relatively protons H-3 and H-4 could be determined by the axial proton to the equatorial proton  $^3J$  coupling constant 5 Hz, indicates that the hydrogen atoms were located on identical sides with a dihedral angle of  $35.7^\circ$  assignment to the cis-configuration. These data were in accordance with those of di-myo-inosital (**3**) as listed in Table 1<sup>25</sup> (Figures 2–5).

Electronic Circular Dichroism (ECD) spectra of chemical constituents were investigated by application of the Gaussian09 program package. Simulation of the ECD spectra of structures were carried out using a computational method. Molecular structures were demonstrated with DEF at CAM-B3LYP level in methyl alcohol. ECD spectra found minimum-energy and stable conformers for compound **1-3** are shown in Figure 2-3<sup>27</sup>.

Proposed biosynthesis pathway: the shikimate pathway commences with the coupling of Phosphoenolpyruvate (PEP) and D-erythrose 4-phosphate to present the 3-deoxy-D-arabino-heptulosonic acid 7-phosphate (DAHP). The reaction losses of phosphoric acid by enzyme 3-dehydroquinate synthase and  $\text{NAD}^+$ , come after with an intra-molecular aldol condensation reaction, originate carbocyclic intermediate 3-dehydroquinic acid (**A**). The keto-enol tautomerism, it involves the migration of a proton from  $\alpha$ -carbon to carbonyl (**B**). Decarboxylation reaction is via loss of a carboxyl group, followed electrons delocalization and loss of hydrates (**C**), giving the inter-conversion of the enol and keto form (**D**). Oxidation reactions catalyze by the cytochrome P-450-dependent monooxygenase. These are involved in biosynthesis hydroxylations to give hydroxyls group (**F**). The reduced form NADPH is conveniently regarded as hydride-donating reducing agents. These reductions reactions are the intermediate carbonyl prior give to



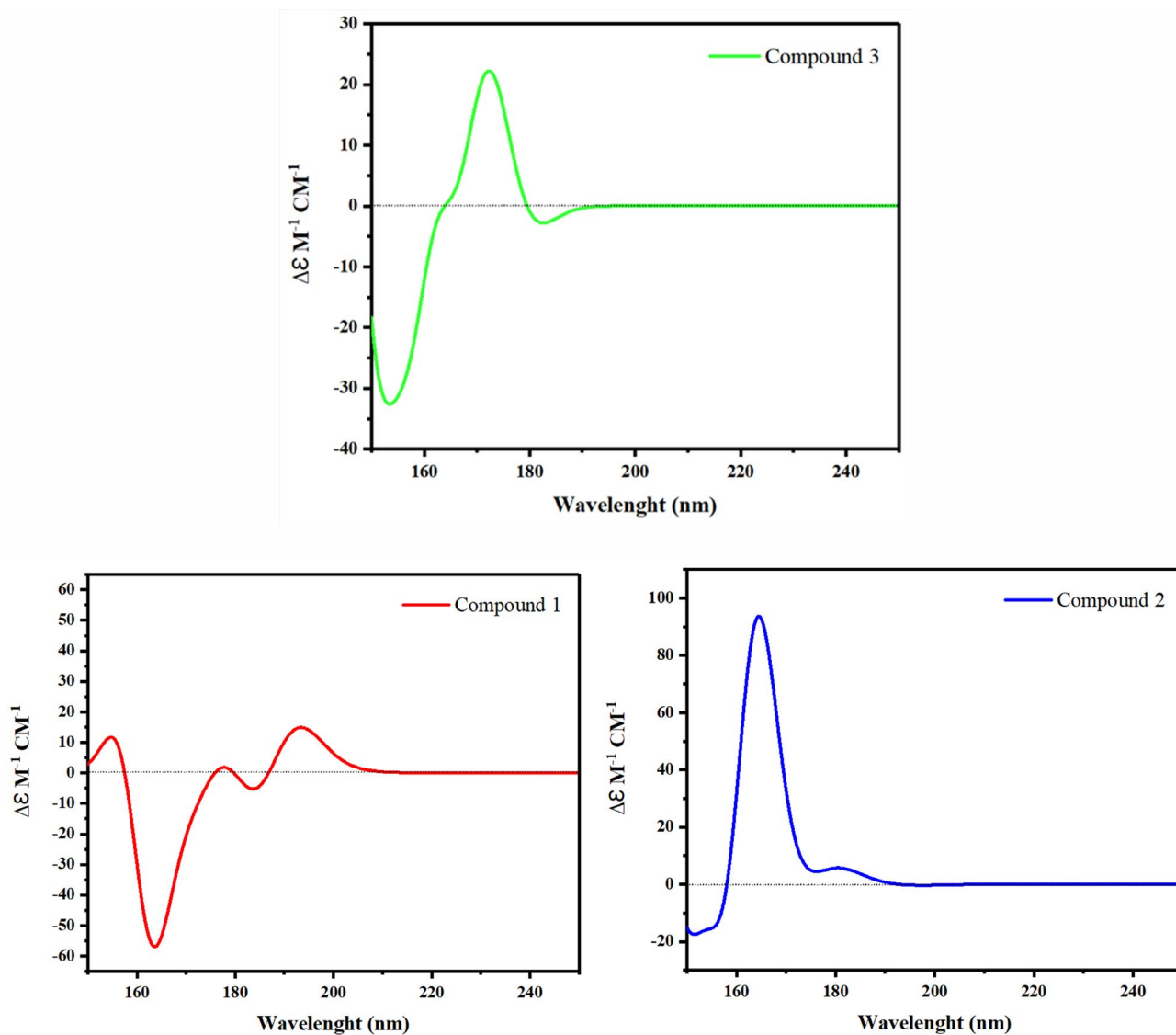


**Figure 3.** Calculated ECD spectrum of compound 1-3 (measured in MeOH).

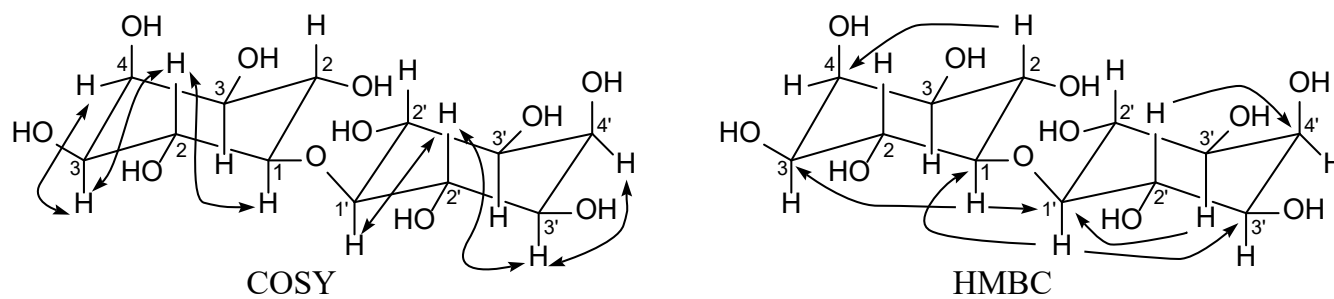


**Figure 4.** Selected COSY and HMBC correlations of compound 3.

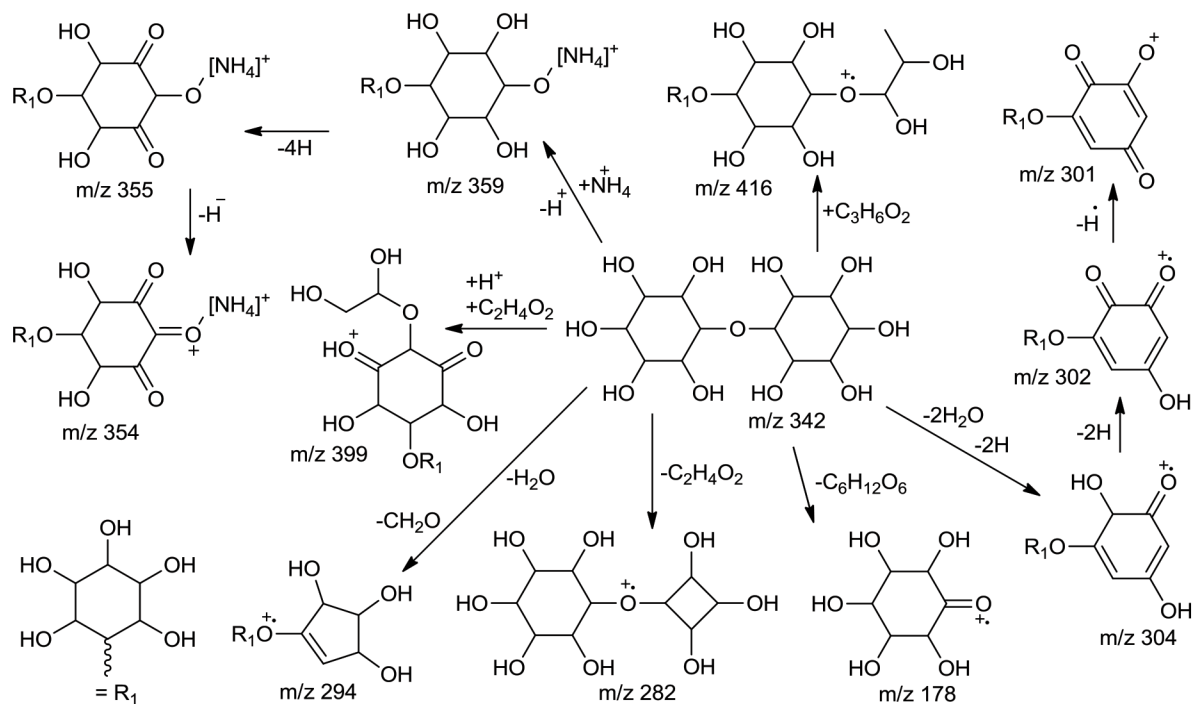


**Figure 5.** The mass spectra fragmentation of compound 3.

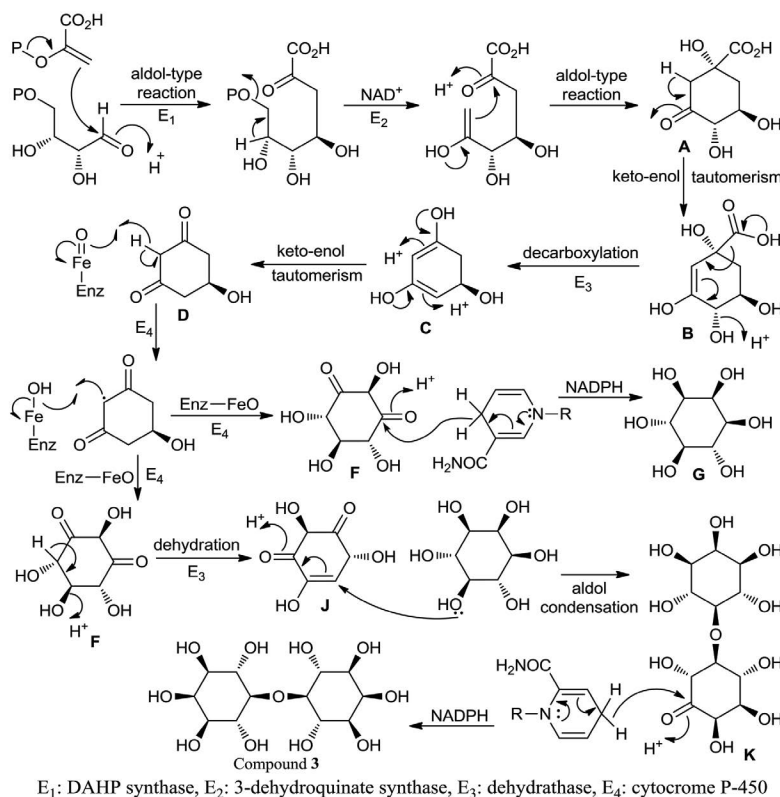


**Figure 6.** Proposed biosynthesis pathway of compound.

the alcohols (G). Elimination of a hydrate from F to give  $\alpha$ ,  $\beta$ -unsaturated carbonyl intermediate (J). Finally, reaction of the intermediate G and J previous to the aldol condensation reaction occurrence (K) and followed reduction with NADPH, leading to constituent of di-myoinositol (3)<sup>26</sup> (Figure 6).

## 5. Conclusion

The new compound of di-myoinositol was successfully extracted, isolated and purified from crude methanol extract, included two known compounds namely stigmasterol and octamethylcyclohexane-1,4-dione from crude n-hexane and ethyl ethanoate extracts of *H. integrifolia*.

## 6. Acknowledgements

We thank the Department of Chemistry, Center for Innovation in Chemistry, Faculty of Science and Graduate School, Chiang Mai University and Lampang Rajabhat University, for science lab, facility and research fund support.

## 7. References

1. Wheeler EA, Manchester SR. Review of the wood anatomy of extant Ulmaceae as context for new reports of late Eocene Ulmus woods. *Bulletin of Geography*. 2007; 82 (4):329–42. <https://doi.org/10.3140/bull.geosci.2007.04.329>
2. Durga N, Paarakh PM. *Holoptelea integrifolia* (Roxb.) Planch-a review. *Pharmaceutical Journal*. 2011; 2:544–57.
3. Sharma J, Singh V. *Holoptelea integrifolia*: An Overview. *European Journal of Applied Sciences*. 2012; 4(1):42–6.
4. Saxena K. Review on study of various extract of part of *Holoptelea integrifolia* and its activity. *International Journal of Pharmaceutical Research and Development*. 2012; 4(03):90–95.
5. Pramod SG, Jayanthi MK, Reddy PC. A study to evaluate and compare the anti-inflammatory activity of ethanolic and aqueous extract of *Holoptelea integrifolia* leaves on acute inflammatory models. *International Journal of Basic & Clinical Pharmacology*. 2016; 5(5):1780–4. <https://doi.org/10.18203/2319-2003.ijbcp20162870>
6. Lalan BK, Hiray RS, Ghonane BB. Evaluation of analgesic and anti-inflammatory activity of extract of *Holoptelea integrifolia* and *Argyreia speciosa* in animal models. *Journal of Clinic and Diagnostic Research*. 2015; 9(7):01–04. <https://doi.org/10.7860/JCDR/2015/12059.6200>. PMID:26393140. PMCid:PMC4572971
7. Lakshmi KS, Shrinivas SS, Rajesh T, Chitra V. Antitumour activity of ethanolic extract of leaves of *Holoptelea integrifolia* on Dalton's ascetic lymphoma in Swiss albino mice. *International Journal of Green Pharmacy*. 2010; 44–7. <https://doi.org/10.4103/0973-8258.62164>
8. Sharma MC, Nigam VK, Behera B, Kachhawa JBS. Antimicrobial activity of aqueous extract of *Holoptelea integrifolia* (Roxb.) leaves: An in vitro study. *Pharmacologyonline*. 2009; 1:155–9.
9. Manoj KT, Prasad N. Antidiabetic activity of seed extract of *Holoptelea integrifolia* in streptozotocin induced diabetic rats. *International Journal of Pharma and Bio Sciences*. 2016; 6(2):161–70.
10. Hemamalini K, Rajani A, Vijusha M, Kavaya SK. Screening of behavioral, muscle coordination anxiolytic activities of methanolic extract of *Holoptelea integrifolia* (Roxb.). *International Research Journal of Pharmacy*. 2013; 4(11):90–4. <https://doi.org/10.7897/2230-8407.041120>
11. Reddy BS, Reddy RKK, Naidu VGM, Madhusudhana K, Agwane SB, Ramakrishna S, Diwan PV. Evaluation of antimicrobial, antioxidant and wound-healing potentials of *Holoptelea integrifolia*. *Journal of Ethnopharmacology*. 2008; 115:249–56. <https://doi.org/10.1016/j.jep.2007.09.031>. PMID:18037253
12. Ganie SA, Yadav SS. FT-IR Spectroscopic analysis of *Holoptelea integrifolia* (Roxb.) planch seed extracts and their antibacterial activity. *Research Journal of Medicinal Plant*. 2015; 9(8):417–26. <https://doi.org/10.3923/rjmp.2015.417.426>
13. Sandhar HK, Kaur M, Tiwari P, Salhan TM, Sharma P, Prasher S, Kumar B. Chemistry and medicinal properties of *Holoptelea integrifolia*. *International Journal of Drug Development and Research*. 2011; 3(1):06–11.
14. Sutar RC, Kasture SB, Kalaichelvan VK. Finger printing analysis of the flavonoids from *Holoptelea integrifolia* (Roxb.) Planch leaves using HPTLC analysis. *Journal of Pharmaceutical and Biomedical Analysis*. 2014; 3(3):80–5.
15. Khalid S, Rizwan GH, Perveen R, Abrar H, Shareef H, Fatima K, Ahmed M. Medicinal importance of *Holoptelea integrifolia* (Roxb.) Planch-Its biological and pharmacological activities. *Natural Product Research*. 2013; 2(1):1–4. <https://doi.org/10.4172/2329-6836.1000124>
16. Durga N, Paarakh PM, Vedamurthy AB. Isolation of phytoconstituents from the stem barks of *Holoptelea integrifolia* (Roxb.) Planch. *Journal of Pharmacy Research*. 2012; 5(1):532–3.
17. Saxena K, Irechhaiya R, Dixit VK. Analytical and medicinal properties of leaves of *Holoptelea integrifolia*. *International Journal of Drug Development and Research*. 2013; 5(2):195–201.



18. Ahmed M, Rizwani GH, Mohammed FV, Mahmood I, Ahmed VU, Mahmud S. A triterpenoid antioxidant agents found in *Holoptelea integrifolia* (Roxb.) Planch. *International Journal of Pharma and Bio Sciences*. 2013; 3(1):63–7.
19. Kumar D, Kumar K, Gupta J, Bishnoi N, Kumar S. A mini review on chemistry and biology of *Holoptelea integrifolia* (Roxb.) Planch (Ulmaceae). *Asian Pacific Journal of Tropical Biomedicine*. 2012; S1200–5. [https://doi.org/10.1016/S2221-1691\(12\)60384-0](https://doi.org/10.1016/S2221-1691(12)60384-0)
20. Chaturvedula VSP, Prakash I. Isolation of Stigmasterol and  $\beta$ -Sitosterol from the dichloromethane extract of *Rubus suavissimus*. *Current Pharmaceutical*. 2012; 1(9):239–42. <https://doi.org/10.3329/icpj.v1i9.11613>
21. Egawa T, Rosario AD, Morris K, Laane J. Vibrational frequencies and conformational stability of 1,4-cyclohexanedione in the gas phase as studied by Infrared and Raman spectroscopy and ab initio calculations. *Journal of Physical Chemistry A*. 1997; 101:8783–7. <https://doi.org/10.1021/jp971339j>
22. Shen Q, Samdal S. The molecular structures and conformational compositions of 1,3-cyclohexanedione and 1,4-cyclohexanedione as determined by gas-phase electron diffraction and theoretical calculation. *Journal of Molecular Structure*. 2011; 1005:156–60. <https://doi.org/10.1016/j.molstruc.2011.08.043>
23. Johnson PY, Jacobs I. The reaction of organozinc reagents with bis (N-Butoxymethyl)-t-butylamine. *Synthetic Communications*. 1974; 4:51–6. <https://doi.org/10.1080/00397917408062054>
24. Haasnoot CAG, Leeuw FAAMD, Leeuw HPMD, Altona C. The relationship between proton-proton NMR coupling constants and substituent electronegativities. *Organic Magnetic Resonance*. 1981; 15(1):43–52. <https://doi.org/10.1002/mrc.1270150111>
25. Riley AM, Laude AJ, Taylor CW, Potter BVL. Dimers of D-myo-Inositol 1,4,5-trisphosphate: Design, synthesis and interaction with Ins(1,4,5)P<sub>3</sub> receptors. *Biochemistry*. 2004; 15:278–89. <https://doi.org/10.1021/bc034214s>. PMID:15025523
26. Dewick PM. Medicinal natural products a biosynthetic approach. John Wiley & Sons, LTD. 3rd; 2002. <https://doi.org/10.1002/0470846275>
27. Padula D, Pescitelli G. How and how much molecular conformation affects electronic circular dichroism: the case of 1,1-diarylcarbinols. *Molecules*. 2018; 23(128):1–14. <https://doi.org/10.3390/molecules23010128>. PMID:29315220. PMCID:PMC6017593